Proceedings of the 15th Annual IEEE International
Conference on Nano/Micro Engineered and Molecular Systems
September 27-30, 2020

AC Electrothermal Flow-Enhanced, Label-Free Immunosensor for Rapid Electrochemical Sensing

Jiran Li[1] and Peter B. Lillehoj*[1,2]

Abstract— **We report a label-free immunosensor employing AC electrothermal flow- (ACEF-) induced mixing for rapid electrochemical measurements of protein biomarkers. Compared with conventional immunoassays that require long (> 1 hr) incubation periods, ACEF-induced mixing significantly reduces the time required for immunocomplex formation while also enhancing the detection sensitivity. Numerical simulations and experimental studies were performed to validate the ACEF mixing approach, and optimize the ACEF operating parameters. Through cyclic voltammetry and fluorescence imaging, we show that ACEF mixing enhances antigen-antibody binding resulting in improved detection sensitivity compared with incubation-based immunocomplex formation. For proof of concept, this immunosensor was used for quantitative measurements of *Plasmodium falciparum* histidine-rich protein 2 (*Pf*HRP2), a biomarker for malaria infection, in buffer samples, which could be detected from 1 ng/mL – 10,000 ng/mL in < 10 min with excellent specificity.**

I. INTRODUCTION

Enzyme-linked immunosorbent assay (ELISA) and Western Blot are considered gold standard techniques for the detection and quantification of proteins in biological samples. However, these assays require multiple antibody-antigen binding steps involving lengthy (> 1 hr) incubation periods, making them laborious and time-consuming. To address these limitations, researchers have developed electrochemical immunoassays for protein measurements, which are rapid, simple to perform and offer high detection sensitivity [1]. Various techniques have been employed to accelerate the transport of biological species to electrochemical sensors for enhanced immunocomplex formation, including direct current (DC) electrokinetics [2] and alternating current (AC) electrokinetics [3-5]. In both of these methods, a driving potential is applied to planar electrodes immersed in a liquid sample to generate an electric field which causes biomolecules to migrate toward the sensor surface via electrostatic forces. While electrokinetics is useful for manipulating biological species in minute liquid samples, it typically requires high operating voltages which can cause electrolysis, and is highly dependent on the properties (e.g. conductivity) of the fluid and of the biological species.

AC electrothermal flow (ACEF) is an alternative technique for generating microflows in which an AC electrical field is applied to planar electrodes, resulting in non-uniform Joule heating of the liquid. The resulting temperature gradient generates thermally driven fluid forces giving rise to swirling flows in the sample (Fig. 1a). In contrast to electrokinetic-driven microflows, ACEF is compatible with biological fluids with high ionic strengths and enables greater control over fluid motion. Theoretical and experimental studies by Ramos et al. showed that the magnitude of electrothermally induced fluid flow is dependent on the AC electric field frequency, voltage, and conductivity of the medium [6]. Computational and experimental studies by Lu et al. also revealed the essential role of buoyancy force in long-range ACEF motion in microchannels [7]. Numerical studies by Sigurdson et al. further showed that electrothermally induced micro-stirring inside microchannels could improve antigen-antibody binding for flow-through assays [8]. Prior reports have also demonstrated the use of ACEF for enhanced electrochemical detection of nucleic acids [9] and enhanced capacitive sensing of proteins [10].

Here, we demonstrate for the first time the use of ACEF mixing for enhanced electrochemical detection of protein biomarkers. Numerical simulations were performed to study the effects of ACEF for a three-electrode configuration commonly used for electrochemical sensing, and to optimize the ACEF operating parameters. Experiments were performed to evaluate the effectiveness of ACEF mixing for enhanced immunocomplex formation and electrochemical sensing. Lastly, we demonstrate the functionality of this immunosensor by performing measurements of *Plasmodium falciparum* histidine-rich protein 2 (*Pf*HRP2) in buffer samples, which could be detected from 1 ng/mL – 10,000 ng/mL in < 10 min.

II. METHODS AND MATERIALS

A. Numerical Simulations

Numerical simulations were performed using COMSOL Multiphysics® software by coupling AC electric field, heat transfer and analyte transport to obtain the concentration profile in a liquid droplet with and without ACEF mixing. The electrothermal force induced by gradients of permittivity ε and conductivity σ can be written as [6]:

$$\vec{F}_E = -0.5\left[\left(\frac{\nabla\sigma}{\sigma} - \frac{\nabla\varepsilon}{\varepsilon}\right)\vec{E}\frac{\varepsilon\vec{E}}{1+(\omega\tau)^2} + 0.5\left|\vec{E}\right|^2\nabla\varepsilon\right] \quad (1)$$

where $\tau=\varepsilon/\sigma$ is the charge relaxation time of the fluid, $\vec{E}$ is the electric field, and ω is the frequency of the AC electric field. In this model, the buoyancy force generated by the density gradient was considered and is denoted by:

$$\vec{F}_B = \rho_E \boldsymbol{g} \quad (2)$$

where ρ_E is the instantaneous density of the fluid. A first-order Langmuir adsorption model was used to describe the

[1] Department of Mechanical Engineering, Rice University, Houston, TX, USA.
[2] Department of Bioengineering, Rice University, Houston, TX, USA.
*Contacting Author: Peter B Lillehoj is with the Departments of Mechanical Engineering and Bioengineering, Rice University, Houston, TX, USA (phone: +1-713-487-7344; e-mail: lillehoj@rice.edu).

978-1-7281-7230-9/20/$31.00 © 2020 IEEE

binding reaction between the antigen and surface-immobilized antibody. The time rate of change of analyte binding ∂Ag/∂t was set equal to the rate of association minus the rate of dissociation, which can be defined by the following kinetics equation:

$$\frac{\partial Ag}{\partial t} = k_{on} Ag(Ab - Ag_{AB}) - k_{off} Ag_{AB} \quad (3)$$

where Ag is the concentration of antigen on the sensor surface, Ab is the concentration of free antibody, Ag_{AB} is the concentration of the antigen-antibody complex, and k_{on} and k_{off} are the association and dissociation rate constants, respectively.

B. Biochemicals and Reagents

Hexaaminеruthenium(III) chloride ($Ru(NH_3)_6^{3+}$), dimethyl sulfoxide (DMSO), phosphate-buffered saline (PBS, pH 7.4), (ethylenedinitrilo)tetraacetic acid (EDTA), 2-Iminothiolane hydrochloride, ethanolamine, N-(3-Dimethylaminopropyl)-N′-ethylcarbodiimide (EDC), N-Hydroxysuccinimide (NHS), latex beads (2.0 µm, carboxylate-modified polystyrene, fluorescent red) were purchased from Sigma-Aldrich (St Louis, MO). Deionized (DI) water was generated using a Smart2Pure water purification system. StabilCoat® Immunoassay Stabilizer was purchased from SurModics, Inc. (Eden Prairie, MN). Mouse monoclonal anti-*Pf*HRP2 IgG was purchased from ICL, Inc. (Portland, OR). Recombinant *P. falciparum* histidine-rich protein 2 (*Pf*HRP2), *P. falciparum* lactate dehydrogenase (*Pf*LDH), and pan-Plasmodium aldolase antigen were purchased from CTK Biotech (San Diego, CA). Poly(methyl methacrylate) (PMMA) and polyester film (PET) were purchased from McMaster-Carr (Elmhurst, IL).

C. Sensor Fabrication and Antibody Immobilization

The electrochemical sensor, consisting of a working electrode (WE), reference electrode (RE) and counter electrode (CE), was fabricated via metal deposition through a custom shadow mask on PMMA. Chromium and gold were sequentially evaporated with thicknesses of 15 nm and 80 nm, respectively using an EnerJet Evaporator. PET film was cut into circular wells using a CO_2 laser cutter (Universal Laser Systems, Scottsdale, AZ) and attached to the sensors using double-sided adhesive.

Anti-*Pf*HRP2 IgG was thiolated (-SH) by incubating 400 µL of 100 µg/mL anti-*Pf*HRP2 IgG with 20-fold molar excess of 2-iminothiolane in PBS containing 2 mM EDTA for 1 hr at room temperature, followed by centrifugation for 25 min at 12,000 rpm to remove excess reagent. Immobilization of the capture antibody to the WE was achieved by incubating 5 µL of thiolated anti-*Pf*HRP2 IgG at 200 µg/mL for 2 hr at room temperature, followed by rinsing with PBS and drying with purified N_2. StabilCoat stabilizer solution was dispensed and dried on the WE to passivate the surface and enhance the stability of the immobilized antibody. Sensors were stored at room temperature in a desiccator (< 30% RH) and used within one week.

D. Assessing Immunocomplex Formation Using Fluorescence Imaging

Anti-*Pf*HRP2 IgM was labeled with fluorescent latex beads using a two-step EDC/Sulfo NHS covalent coupling protocol (EMD Millipore). Briefly, 20 µL of latex beads (at 10% w/v) was repeatedly purified by centrifugation at 10,000 rpm for 5 min in a low-protein binding Eppendorf tube (Hauppauge, NY). 200 mM of EDC and Sulfo-NHS were added to the washed beads which were subsequently reconstituted in 50 mM of MES buffer and incubated for 30 min at room temperature. Functionalized beads were incubated with anti-*Pf*HRP2 IgM (10 µL at 2 mg/mL) for 2.5 hr, followed by pelleting, resuspension in 25% StabilCoat solution and incubation at room temperature for 2 hr. IgM-bead conjugates (2% w/v) were used immediately or stored at 4 °C for up to one week.

Sensors functionalized with antigen-antibody complexes were incubated with 100 µL of 10-fold diluted IgM-bead conjugate solution for 2 hr, followed by rinsing with PBS for three times. Fluorescence images of sensors were obtained using a Nikon CiS microscope with a Coolsnap HQ2 cooled CCD camera.

E. ACEF Mixing and Electrochemical Measurements

Fig. 1b shows the experimental setup for performing ACEF mixing and electrochemical measurements. 60 µL of sample was first dispensed on the sensor. ACEF mixing was performed by applying an 8 V_{pp} (peak-to-peak) square wave potential at 200 kHz between the WE and CE for 5 min using a function generator (Tabor Electronics, Irvine CA). The sensor was rinsed in PBS followed by the application of a 200 µM $Ru(NH_3)_6^{3+}$ solution. Cyclic voltammetry (CV) and square wave voltammetry (SWV) were performed using a CHI 620A electrochemical analyzer (CH Instruments, Austin, TX). SWV was performed from 0 V to -0.6 V, at a frequency of 100 Hz, amplitude of 15 mV and sensitivity of 500 nA.

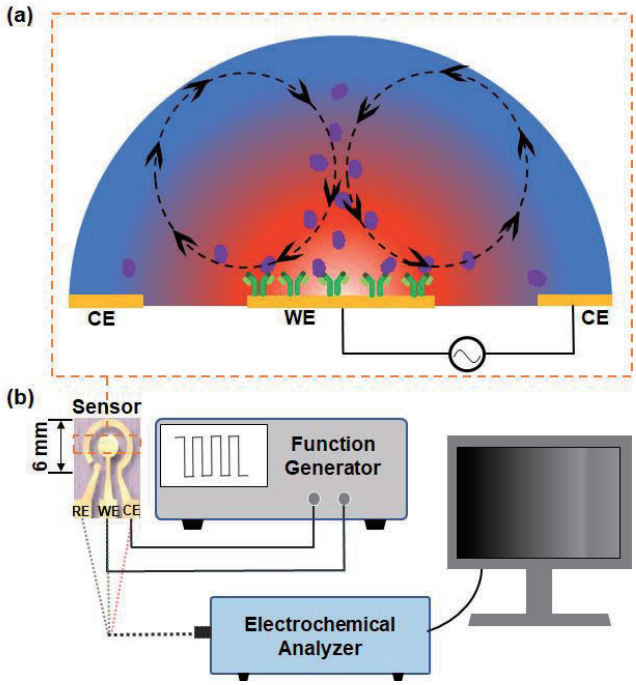

Figure 1. Schematic illustrations of ACEF-induced mixing (a), and the experimental setup for performing ACEF mixing and electrochemical measurements (b).

III. RESULTS

A. Electrochemical Sensing Scheme

A schematic of the electrochemical sensing scheme is shown in Fig. 2. The WE is coated with anti-*Pf*HRP2 IgG. In the absence of the target *Pf*HRP2 antigen, the redox species can easily pass through the electrode surface, resulting in fast electron transfer and a large electrochemical current (Fig. 2a). If *Pf*HRP2 antigen is present in the sample, it binds to the surface-immobilized anti-*Pf*HRP2 IgG, forming a robust immunocomplex layer which hinders access of the redox species to the electrode surface (Fig. 2b). Based on this scheme, the magnitude of the electrochemical current is inversely proportional to the antigen concentration where samples containing higher concentrations of *Pf*HRP2 will generate a lower detection signal (Fig. 2c).

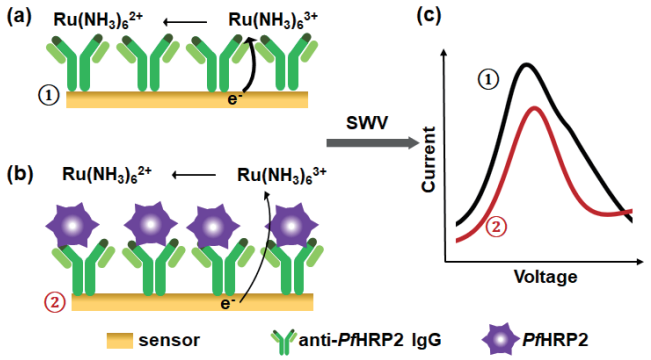

Figure 2. Schematic illustration of the label-free electrochemical sensing scheme in the absence (a) and presence (b) of the target *Pf*HRP2 antigen, and the corresponding SWV response curves (c).

B. Numerical Simulation Results of ACEF Mixing

The results obtained from our numerical simulations show that electrothermal forces induce swirling fluid motion within the liquid droplet, which facilitates the transport of biological species from the bulk solution to the sensor surface, thereby enhancing antibody-antigen binding (Fig. 3a). In contrast, the analyte concentration is largely uniform in the droplet without ACEF mixing, where the transport of biological species to the sensor surface is limited by diffusion (Fig. 3b). Numerical simulations were also used to obtain optimized ACEF operating parameters, where an applied voltage of 8 V_{pp} at 200 kHz generated a 5-fold increase in antigen-antibody binding compared to the diffusion limited condition at 0 V_{pp} (Fig. 3c).

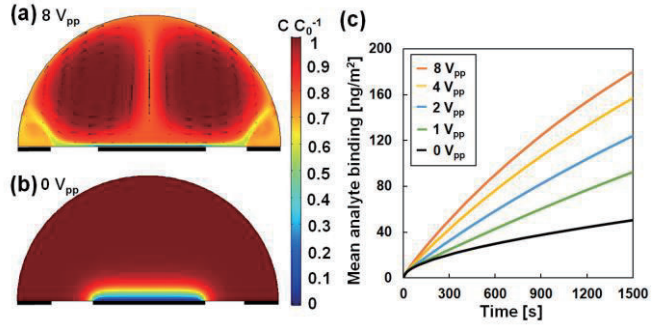

Figure 3. 2D simulation results of the concentration profile in a liquid droplet with ACEF mixing at 8 V_{pp} and 200 kHz (a), or with diffusion for 5 min (b). (c) Concentration of analyte binding *vs*. time with ACEF mixing at varying potentials and 200 kHz.

C. *ACEF Mixing for Enhanced Immunocomplex Formation*

To validate the effectiveness of ACEF mixing for enhanced immunocomplex formation, CV measurements were performed with ACEF mixing or 2 hr incubation using PBS samples spiked with 10 µg/mL of *Pf*HRP2 and non-spiked PBS samples. As shown in curves i and ii of Fig. 4, large voltammetric currents are generated with PBS samples without *Pf*HRP2 due to enhanced electron transfer between the redox species and the sensor surface. The larger voltammetric current generated with ACEF mixing is likely due to the removal of nonspecific species on the sensor surface via electrothermally induced fluid motion, which results in a higher background signal. This phenomenon was also observed by Sin et al. when employing ACEF mixing for electrochemical detection of nucleic acids [9]. Measurements of the *Pf*HRP2-spiked sample with 2 hr incubation resulted in a moderate suppression of the electrochemical current and slight shift in the reduction peak (curve iv in Fig. 4), indicating minimal immunocomplex formation. However, the voltammetric current generated with ACEF mixing is significant diminished (curve iii in Fig. 4) due to the formation of a robust immunocomplex layer, which greatly inhibits the transport of redox species to the sensor surface.

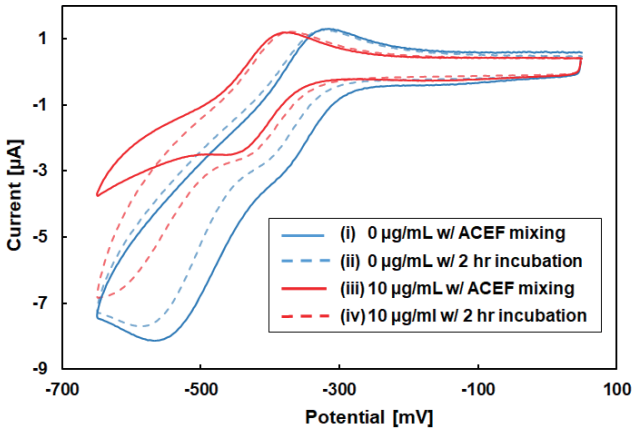

Figure. 4. Cyclic voltammograms (50 mV/s) of non-spiked PBS samples with ACEF mixing (i) or with 2 hr incubation (ii). Cyclic voltammograms of PBS samples spiked with 10 µg/mL of *Pf*HRP2 with ACEF mixing (iii) or with 2 hr incubation (iv). ACEF mixing was performed with the following parameters: 8 V_{pp}/200 kHz/5 min.

The capability of ACEF mixing to enhance the formation of antigen-antibody complexes on the sensor surface was further evaluated by performing fluorescence imaging of sensors with and without ACEF mixing that were subsequently incubated with anti-*Pf*HRP2 IgM-fluorescent bead conjugates. As shown in Fig. 5a, the sensor employing ACEF mixing with the *Pf*HRP2-spiked sample was largely covered with immobilized IgM-bead conjugates indicating broad immunocomplex formation. In contrast, incubating the *Pf*HRP2-spiked sample on the sensor for 2 hr resulted in a significantly lower concentration of immobilized IgM-bead conjugates (Fig. 5b), indicating minimal immunocomplex formation. Negligible fluorescence signals were observed for

sensors employing ACEF mixing (Fig. 5c) or 2 hr incubation (Fig. 5d) using non-spiked PBS samples, which can be attributed to non-specific binding of IgM-bead conjugates (Fig. 5c).

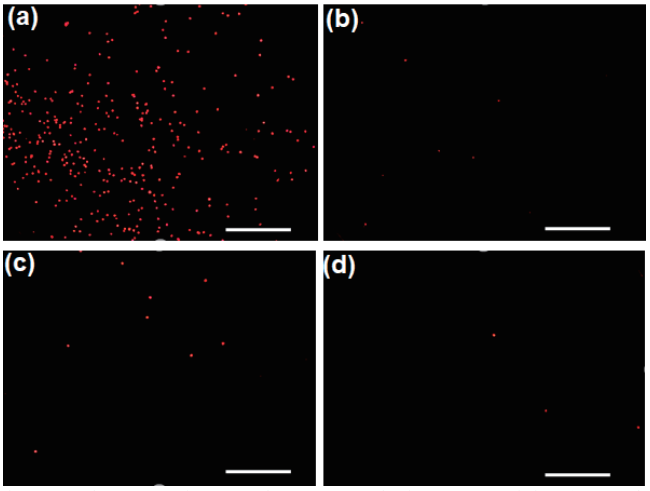

Figure 5. Fluorescent images of sensors employing ACEF mixing (a) or 2 hr incubation (b) with 10 µg/mL of *Pf*HRP2 in PBS. Florescent images of sensors employing ACEF mixing (c) or 2 hr incubation of non-spiked PBS (d). Scale bars, 100 µm.

D. Optimization of ACEF Parameters

Several ACEF operating parameters, such as the applied potential and mixing duration, were optimized to enhance the analytical performance of the immunosensor. Based on prior studies showing optimal ACEF generation at 200 kHz [9, 11], this frequency was selected for ACEF mixing in this work. SWV measurements of PBS samples spiked with and without *Pf*HRP2 were performed at varying potentials from 1 V_{pp} to 10 V_{pp}. SWV measurements of *Pf*HRP2-spiked PBS samples incubated for 2 hr were also performed for comparison. As shown in Fig. 6a, the background current steadily increases with increasing potentials from 1 V_{pp} to 8 V_{pp} while the detection current for the *Pf*HRP2-spiked samples increases only slightly. While a slightly higher background current is generated at 10 V_{pp} compared with 8 V_{pp}, the change in current before and after antigen-antibody complex formation (ΔI) is ~20% lower. Therefore, a potential of 8 V_{pp} was selected to obtain the maximum ΔI. Furthermore, ΔI at 8 V_{pp} is ~4-fold larger compared with ΔI for sensors employing 2 hr incubation. The ACEF mixing time was optimized by performing SWV measurements of PBS samples spiked with or without *Pf*HRP2 employing ACEF at varying durations. As shown in Fig. 6b, longer mixing times generated larger ΔI values from 0 min to 5 min. However, with 8 min of ACEF mixing, ΔI significantly decreased which is likely due to the removal of immobilized proteins and/or the deformation of antigen-antibody complexes resulting from excessive heating. Based on these results, 5 min was selected as the optimal ACEF mixing duration.

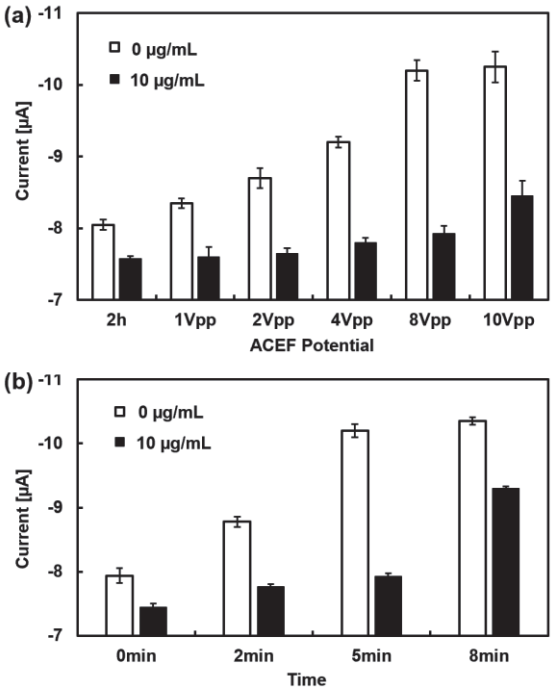

Figure. 6. (a) SWV measurements of PBS samples spiked with or without 10 µg/mL of *Pf*HRP2 at varying ACEF potentials for 5 min. (b) SWV measurements of PBS samples spiked with or without 10 µg/mL of *Pf*HPR2 employing ACEF mixing (8 V_{pp}) at varying mixing durations. Each bar represents the mean ± standard deviation (SD) of three separate measurements obtained using new sensors.

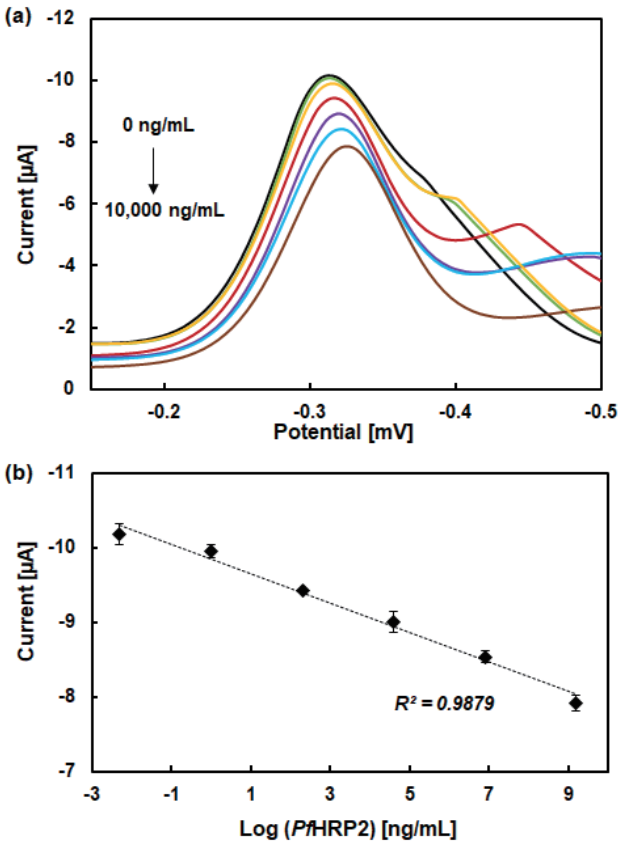

Figure 7. (a) Square wave voltammograms of PBS samples containing increasing concentrations of *Pf*HRP2. (b) Calibration plot based on the peak currents of the SWV curves obtained in panel a. Each data point represents the mean ± SD of three separate measurements obtained using new sensors.

E. Assay Sensitivity and Specificity

The sensitivity of this immunosensor was evaluated by performing measurements of PBS samples spiked with

*Pf*HRP2 from 1 ng/mL to 10,000 ng/mL. Square wave voltammograms at different *Pf*HRP2 concentrations and the corresponding calibration curve are shown in Fig. 7a and b, respectively. The observed response of the immunosensor is consistent with the predicted response based on the sensing scheme where the magnitude of the peak current is inversely proportional to the *Pf*HRP2 concentration. Samples with larger concentrations of *Pf*HRP2 generate a lower electrochemical current. As shown in Fig. 7a, the lowest concentration that could be detected is 1 ng/mL, which is comparable with other rapid immunosensors [12-14] but with a 100–fold greater detection range. Furthermore, this assay exhibits a linear response over the entire concentration range with a R^2 correlation coefficient of 0.988.

The specificity of this immunosensor was evaluated by measuring PBS samples spiked with *Pf*HRP2 or other common biomarkers for *P. falciparum* infection, including pan-Plasmodium aldolase and *Pf*LDH at 10 µg/mL. As shown in Fig. 8, the electrochemical currents generated from samples containing irrelevant proteins were similar to the non-spiked PBS sample (blank control). In contrast, the electrochemical current of the sample containing *Pf*HRP2 was significantly lower demonstrating that this immunosensor does not exhibit cross reactivity with other *P. falciparum* biomarkers.

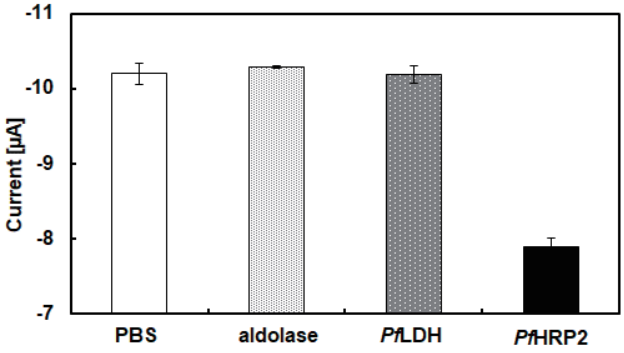

Figure 8. SWV measurements of PBS samples spiked with *Pf*HRP2, *Pf*LDH or pan-Plasmodium aldolase (aldolase), and non-spiked PBS as a blank control. Each bar represents the mean ± SD of three separate measurements obtained using new sensors.

IV. Conclusions

We have demonstrated an ACEF-enhanced label-free immunosensor for rapid electrochemical measurements of protein biomarkers. Through numerical simulations and experimental studies, we showed that ACEF-induced mixing can significantly reduce the time for immunocomplex formation compared with incubation-based antigen-antibody binding while also resulting in a higher detection sensitivity due to electrothermal flow-induced removal of nonspecific species from the sensor surface. Proof of concept was carried out by using this immunosensor for quantitative measurements of *Pf*HRP2, which could be detected from 1 ng/mL – 10,000 ng/mL in < 10 min. Experiments to evaluate the specificity of this platform revealed that it is highly specific to *Pf*HRP2 and does not cross react with other common protein biomarkers associated with *P. falciparum* infection. The speed, simplicity and analytical performance of this ACEF-enhanced label-free immunoassay makes it a promising platform for the detection and quantification of protein biomarkers, particularly for point-of-care applications.

Acknowledgments

This work was funded by the National Institutes of Health (R01AI113257). We thank Prof. Andrew J. Mason for the use of his function generator.

References

[1] D. Grieshaber, R. Mackenzie, J. Vörös, and E. Reimhult, "Electrochemical Biosensors - Sensor Principles and Architectures," *Sensors*, vol. 8, no. 3, pp. 1400–1458, Jul. 2008.

[2] Du, Dan, et al. "Multiplexed Electrochemical Immunoassay of Phosphorylated Proteins Based on Enzyme-Functionalized Gold Nanorod Labels and Electric Field-Driven Acceleration." *Analytical Chemistry*, vol. 83, no. 17, 2011, pp. 6580–6585.

[3] Sanghavi, Bankim J., et al. "Correction: Ultrafast Immunoassays by Coupling Dielectrophoretic Biomarker Enrichment in Nanoslit Channel with Electrochemical Detection on Graphene." *Lab on a Chip*, vol. 15, no. 24, 2015, pp. 4626–4626.

[4] Cheng, I-Fang, et al. "A Rapid Electrochemical Biosensor Based on an AC Electrokinetics Enhanced Immuno-Reaction." *The Analyst*, vol. 138, no. 16, 2013, p. 4656.

[5] Chuang, Cheng-Hsin, et al. "Immunosensor for the Ultrasensitive and Quantitative Detection of Bladder Cancer in Point of Care Testing." *Biosensors and Bioelectronics*, vol. 84, 2016, pp. 126–132., doi:10.1016/j.bios.2015.12.103.

[6] A. Ramos, H. Morgan, N. G. Green, and A. Castellanos, "Ac electrokinetics: a review of forces in microelectrode structures," *Journal of Physics D: Applied Physics*, vol. 31, no. 18, pp. 2338–2353, 1998.

[7] Y. Lu, Q. Ren, T. Liu, S. L. Leung, V. Gau, J. C. Liao, C. L. Chan, and P. K. Wong, "Long-range electrothermal fluid motion in microfluidic systems," *International Journal of Heat and Mass Transfer*, vol. 98, pp. 341–349, 2016.

[8] M. Sigurdson, D. Wang, and C. D. Meinhart, "Electrothermal stirring for heterogeneous immunoassays," *Lab on a Chip*, vol. 5, no. 12, p. 1366, 2005.

[9] M. L. Y. Sin, T. Liu, J. D. Pyne, V. Gau, J. C. Liao, and P. K. Wong, "In Situ Electrokinetic Enhancement for Self-Assembled-Monolayer-Based Electrochemical Biosensing," *Analytical Chemistry*, vol. 84, no. 6, pp. 2702–2707, Jun. 2012.

[10] H. Cui, C. Cheng, X. Lin, J. Wu, J. Chen, S. Eda, and Q. Yuan, "Rapid and sensitive detection of small biomolecule by capacitive sensing and low field AC electrothermal effect," *Sensors and Actuators B: Chemical*, vol. 226, pp. 245–253, 2016.

[11] Y. Lu, T. Liu, A. C. Lamanda, M. L. Y. Sin, V. Gau, J. C. Liao, and P. K. Wong, "AC Electrokinetics of Physiological Fluids for Biomedical Applications," *Journal of Laboratory Automation*, vol. 20, no. 6, pp. 611–620, 2015.

[12] S. Wang, Y. Quan, N. Lee, and I. R. Kennedy, "Rapid Determination of Fumonisin B1in Food Samples by Enzyme-Linked Immunosorbent Assay and Colloidal Gold Immunoassay," *Journal of Agricultural and Food Chemistry*, vol. 54, no. 7, pp. 2491–2495, 2006.

[13] Q. Yang, X. Gong, T. Song, J. Yang, S. Zhu, Y. Li, Y. Cui, Y. Li, B. Zhang, and J. Chang, "Quantum dot-based immunochromatography test strip for rapid, quantitative and sensitive detection of alpha fetoprotein," *Biosensors and Bioelectronics*, vol. 30, no. 1, pp. 145–150, 2011.

[14] G. Liu, H. Chen, H. Peng, S. Song, J. Gao, J. Lu, M. Ding, L. Li, S. Ren, Z. Zou, and C. Fan, "A carbon nanotube-based high-sensitivity electrochemical immunosensor for rapid and portable detection of clenbuterol," *Biosensors and Bioelectronics*, vol. 28, no. 1, pp. 308–313, 2011.